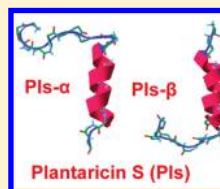ARTICLE

Structure−Activity Relationships of an Antimicrobial Peptide Plantaricin S from Two-Peptide Class IIb Bacteriocins

Wael Soliman,[†] Liru Wang,[‡] Subir Bhattacharjee,[§] and Kamaljit Kaur*,[†]

[†]Faculty of Pharmacy and Pharmaceutical Sciences, University of Alberta, Edmonton, Alberta, T6G 2N8, Canada
[‡]CanBiocin Inc., Edmonton, Alberta, T5J 4P6, Canada
[§]Department of Mechanical Engineering, University of Alberta, Edmonton, Alberta, T6G 2G8, Canada

Ⓢ Supporting Information

ABSTRACT: Class IIb bacteriocins are ribosomally synthesized antimicrobial peptides comprising two different peptides synergistically acting in equal amounts for optimal potency. In this study, we demonstrate for the first time potent (nanomolar) antimicrobial activity of a representative class IIb bacteriocin, plantaricin S (Pls), against four pathogenic Gram-positive bacteria, including *Listeria* monocytogenes. The structure−activity relationships for Pls were studied using activity assays, circular

dichroism (CD), and molecular dynamics (MD) simulations. The two Pls peptides and five Pls derived fragments were synthesized. The CD spectra of the Pls and selected fragments revealed helical conformations in aqueous 2,2,2-trifluoroethanol. The MD simulations showed that when the two Pls peptides are in antiparallel orientation, the helical regions interact and align, mediated by strong attraction between conserved GxxxG/AxxxA motifs. The results strongly correlate with the antimicrobial activity suggesting that helix−helix alignment of the two Pls peptides and interaction between the conserved motifs are crucial for interaction with the target cell membrane.

■ INTRODUCTION

Antimicrobial peptides (AMPs) from lactic acid bacteria (LAB) are potential new sources of antibiotics for treatment against pathogenic and drug-resistant bacterial infections. LAB are Gram-positive organisms that secrete ribosomally synthesized AMPs called bacteriocins.[1,2] Bacteriocins possess potent activity against pathogenic drug-resistant bacteria and have gained recognition as natural food preservatives, additives to animal feed, and potential alternatives to conventional antibiotics.[3−5] Bacteriocins from LAB have been classified into two main groups, lantibiotic (class I) and non-lantibiotic (class II) peptides.[1] Lantibiotic nisin, non-lantibiotic pediocin PA-1, and several other bacteriocins have been approved for use as food preservatives,[2] and the potential of LAB bacteriocins in medical applications has also been demonstrated.[6]

Class II bacteriocins are cationic peptides consisting of unmodified residues. They are synthesized as prepeptides (precursor peptides) that contain an N-terminal leader sequence that is cleaved off by a dedicated ABC transporter to produce the active mature peptide. Class II bacteriocins are heterogeneous and have been further divided into at least four subclasses, IIa, IIb, IIc, and IId. Class IIa bacteriocins are antilisterial peptides that consist of one-peptide systems with conserved N-terminal sequences, whereas class IIb are two-peptide bacteriocins where two different peptides act synergistically in equal amounts for optimal antimicrobial activity.[7,8] The two complementary peptides are generally active at picomolar to nanomolar concentrations when combined together but show no activity (sometimes

low activity) when assayed individually at micromolar concentrations. The two peptides likely display their antibacterial effect by rendering the membrane of sensitive bacteria permeable to small molecules.[9−13]

The first two-peptide bacteriocin, lactococcin G (LcnG-α and LcnG-β), was isolated in 1992, and since then at least 14 more two-peptide bacteriocins have been identified, isolated, and characterized (Table 1).[1] Further, solution conformation and mutagenesis studies have been utilized to elucidate the mechanism of action of these peptides.[14−18] The three-dimensional solution structure of three two-peptide bacteriocins, namely, lactococcin G,[14] plantaricin E/F,[15] and plantaricin J/K,[16] has been reported. The NMR structure in membrane mimicking environments, such as trifluoroethanol (TFE) or DPC micelles, shows that the individual peptides fold into helical conformations. Circular dichroism (CD) studies show that the helical content increases when both the complementary peptides are present together in the solution.[19] This indicates that there could be a direct interaction between the two peptides (α and β pair). In addition, several studies suggest that the two peptides act as a one-functional unit based on the following observations: (i) potent antibacterial activity is produced only when the two peptides combine together; (ii) the genes encoding the two peptides are always adjacent to each other on the same operon; (iii) the two peptides are produced in approximately equal

Table 1. Amino Acid Sequences of a Few Class IIb Two-Peptide Bacteriocins[a]

peptide		amino acid sequence	no. of residues	reference
lactococcin G	LcnG-α	GTWDDI**GQGIG**RVAYWV**GKAMG**NMSDVNQASRINRKKKH	39	14
	LcnG-β	KKWGWLAWVDPAYEFIK**GFGKG**AIKEGNKDKWKNI	35	
plantaricin E/F	PlnE	FNRG**GYNFG**KSVRHVVDAI**GSVAG**IRGILKSIR	33	15
	PlnF	VFHAYSARGVRNNYKSAVGPADWVISAVR**GFIHG**	34	
plantaricin J/K	PlnJ	GAWKNFWSSLRK**GFYDG**EAGRAIRR	25	16
	PlnK	RRSRKNGI**GYAIGYAFG**AVERAVLGGSRDYNK	32	
plantaricin S	Pls-α	RNKLAYNM**GHYAG**KATIFGLAAWALLA	27	22
	Pls-β	KKKKQSWYA**AAGDA**IVSFGEGFLNAW	26	

[a] The GxxxG or AxxxA motifs are marked as bold.

amounts; (iv) there is one immunity protein that confers resistance to producer strains from the antibacterial action of the two-peptides.[20] Thus, the synergistic action of class IIb bacteriocins seems to be due the fact that the complementary peptides interact with each other and form one antibacterial unit rather than separately acting on two different sites on the target cells.

Two-peptide bacteriocins contain one or two conserved GxxxG motifs (Table 1), and these motifs have been proposed to mediate helix−helix interactions between the two complementary peptides. The two glycine residues from the GxxxG motifs are likely on the same side of the helices. This creates flat interaction sites allowing close contact between the two helices with extensive interhelical van der Waals interactions and the formation of stabilizing backbone hydrogen bonds.[17] Further, the two helices get inserted in the target cell membrane to form a transmembrane helix−helix structure that might interact with an integrated membrane protein in a manner similar to what has been shown for class IId lactococcin A and the class IIa pediocin-like bacteriocins.[21] A membrane associated target for class IIb bacteriocins has not been identified so far; however, it has been speculated that a putative lactococcin G receptor mediates the interaction between lactococcin G and lactococcin G immunity protein in a manner similar to what has been reported for class IIa bacteriocins.[8] Beyond this, specific mechanisms of action of these peptides in the disruption of the cell membrane are unclear.

Plantaricin S (Pls), produced by *Lactobacillus plantarum* LPCO10, consists of two peptides Pls-α (27-residue) and Pls-β (26-residue).[22] Both α and β peptides are cationic and hydrophobic in nature, and when present together, the peptides are active against *L. plantarum* 128/2. In order to understand structural features that are important for function and potency, an extensive structure−function analysis of the two-peptide Pls is required. In this study, we have synthesized the wild-type Pls peptides (Pls-α and Pls-β) and five Pls derived fragments. Pls-α derived fragments are based on the presence of (i) the GxxxG motif (fragment α1), (ii) the GxxxG motif and C-terminal helical region (fragment α2), and (iii) the C-terminal helical region (fragment α3). Similarly, fragments from Pls-β contain (i) the AxxxA motif and the helical domain (fragment β4) and (ii) the AxxxA motif, helical domain, and the C terminal acidic residue E20 (fragment β5). The fragments are designed to determine the role of different prominent components in the peptide sequence for antibacterial activity. The potent antibacterial activity of Pls against several pathogenic Gram-positive strains including *Listeria monocytogenes* and examination of the structure−activity relationship in Pls and fragments using activity assays, circular dichroism (CD) spectroscopy, and molecular dynamics (MD) simulations are reported.

Table 2. Amino Acid Sequences of Pls Peptides and Derived Fragments Studied Herein[a]

peptide	amino acid sequence	no. of residues	charge
Pls-α	RNKLAYNX**G**HYA**G**KATIFGLAAWALLA	27	+3
Pls-β	KKKKQSWYA**A**AGD**A**IVSFGEGFLNAW	26	+2
α1	RNKLAYNX**G**HYA**G**KA	15	+3
α2	NX**G**HYA**G**KATIFGLAAWALLA	21	+1
α3	KATIFGLAAWALLA	14	+1
β4	KKKKQSWYA**A**AGD**A**IV	16	+3
β5	KKKKQSWYA**A**AGD**A**IVSFGEG	21	+2

[a] Methionine in Pls sequence is replaced with norleucine (Nle or X). The underlined residues denote the projected helical regions of Pls as inferred from homology modeling and confirmed by secondary structure prediction softwares (see Materials and Methods).

■ MATERIALS AND METHODS

Synthesis and Purification of Peptides. Stepwise synthesis of the wild-type plantaricin S α- and β-peptides was carried out manually on a 0.2 mmol scale of chlorotrityl resin (1.0% DVB cross-linked) following the standard Fmoc solid-phase peptide chemistry as described previously.[23] Fmoc-protected L-amino acids were used, and the following side chain protection was used: Boc (Lys, Trp), tBu (Ser, Thr, Tyr), OtBu (Asp, Glu), Trt (Asn, Gln, His), and Pbf (Arg). A test cleavage was performed after every five residues were coupled and the desired product was confirmed by MALDI-TOF mass spectrometry. Each test peptide was cleaved from the resin with a mixture of 90% TFA, 5% triisopropylsilane, and 5% water for 90 min at room temperature with mechanical shaking. After complete assembly on the resin, the peptides were released from support with concomitant removal of acid-labile side chain protecting groups using the same procedure as used for the test cleavages. The filtrate from the cleavage reactions was collected, combined with TFA washes (3 × 2 min, 1 mL), and concentrated in vacuum. Cold diethyl ether (∼15 mL) was added to precipitate the crude cleaved peptide. After trituration for 2 min, the peptides were collected upon centrifugation and decantation of the ether. The crude peptides were dissolved in 10−20% aqueous acetonitrile and purified on a semipreparative VYDAC C8 reversed-phase HPLC column (1 cm × 25 cm, 5 μm) using an isopropanol/water gradient in the presence of 0.05% TFA. The details of the gradient elution method used for the purification of each peptide are listed in Table S1 (Supporting Information). Purity of the peptides was confirmed by analytical reversed-phase HPLC and MALDI-TOF mass spectrometry. The purity of the peptides was verified to be greater than 95% by analytical reverse-phase chromatography. Peptide fragments (α1−β5, Table 2), ranging in length 14−21 residues, were prepared using automatic peptide synthesizer (Advanced ChemTech MPS 357, Louisville, KY, U.S.) using DIC and HOBt as coupling agents. Met8 of Pls-α

and the fragments (α1 and α2) was replaced with Nle to avoid any oxidation problem. The synthetic Pls-α with M8X mutation is called "wild type Pls-α" throughout the manuscript.

Antimicrobial Activity. Seven strains, namely, *Carnobacteriocin divergens* LV13 (grown in APT broth at 25 °C), *Lactobacillus plantarum* WCSFI (APT broth, 37 °C), *Lactobacillus fermentrum* 14931 (APT broth 37 °C), *Enterococcus faecalis* 19433 (APT broth, 25 °C), *Enterococcus faecium* 19434 (APT broth, 25 °C), *Listeria monocytogenes* NCTC 5105.3 (TSYBE, 37 °C), and *Listeria monocytogenes* CDC 7762 (TSYBE, 37 °C) were used as indicators for the activity assay. All indicator strains were obtained from the culture collection of CanBiocin Inc. (Edmonton, Alberta, Canada). Wild-type Pls and peptide fragments (α1−β5) in combination with the complementary wild-type peptide were assayed for antimicrobial activity. Activity was quantified using a microtiter plate assay system as described previously.[24,25] Culture media, the peptide combination (at 2-fold dilutions), and the indicator organism were added to a final volume of 200 μL in each well. Stationary phase cultures of the indicator organisms were diluted 1:100 before adding to the microtiter plates. The microtiter plates were then incubated overnight at the specified temperature before the growth inhibition was measured spectrophotometrically at 600 nm using a microplate reader (TECAN, Männedorf, Switzerland). The minimum inhibitory concentration (MIC) was defined as the total amount of peptides (the sum of both peptides in 1:1 ratio concentrations) that inhibited the growth by 50%. Competition experiments were performed similarly where a 200 μL volume of culture medium, wild-type Pls (slightly above its MIC), various amounts of peptide fragments at 2-fold dilutions, and the indicator strain (*C. divergens* LV13, diluted 1:100) were added to each well of the microtiter plate. The microtiter plate culture was incubated overnight at 25 °C, after which the growth of the indicator strain was measured spectrophotometrically at 600 nm.

CD Spectroscopy. The circular dichrosim (CD) measurements were made on Olis CD spectrometer (GA, U.S.) at 25 °C in a thermally controlled quartz cell with a 0.02 cm path length over 190−260 nm. The samples were prepared by dissolving the peptides in 50% TFE/water mixture containing 0.05% TFA. The final peptide concentration for the CD measurements was 50 μM. Data were collected every 0.05 nm and were the average of eight scans. The bandwidth was set at 1.0 nm and the sensitivity at 50 mdeg. The response time was 0.25 s. In all cases, baseline scans of aqueous buffer were subtracted from the experimental readings. The CD data were normalized and expressed in terms of mean residue ellipticity (deg cm^2 dmol^{-1}). CD spectra were analyzed using quantitative curve fitting using the CDPro software analysis program as described previously.[26]

Modeling and Simulation Methods. The primary amino acid sequence of both Pls peptides (α and β) has been reported previously.[22] Sequence alignment between the primary structure of Pls and other class IIb bacteriocins with reported structures was done using EMBOSS pairwise alignment algorithms.[27] Among the reported NMR structures, plantaricin E (PlnE, PDB code 2JUI) and lactococcin G (LcnG-β, PDB code 2JPK) showed high sequence similarity with Pls-α and -β peptides, respectively.[14,15] Multiple amino acid sequence alignments and initial homology-based structures for Pls-α and -β were obtained using the "magic fit" module of Swiss-PdbViewer 4.[28] These homology-based structures were chosen as the starting structures for subsequent MD simulations.

Simulation Box Construction. A mixed lipid bilayer made of anionic POPG and zwitterionic POPE (3:1, POPG/POPE) homogenously distributed in a bilayer structure (74 per leaflet) was used to mimic the cell membranes of Gram-positive bacteria. The analyses of major phospholipid components of several Gram-positive bacteria show that they contain mostly PG and PE lipids with the former reaching up to 80%.[29−31] The bilayer was created using the PDB coordinates of POPG[32] and POPE[33] molecules as described previously.[34]

The system was set up by placing the two Pls (α and β) peptides in either an antiparallel or a parallel orientation. In the first system (simulation α/β-1), the α and β peptides were placed in an antiparallel orientation in the z direction perpendicular to the plane of the bilayer. In this orientation, the C-terminal of the α-peptide and N-terminal of the β-peptide were touching the upper leaflet of the bilayer. The starting configurations were generated by adding SPC water molecules on both sides of the bilayer. Sufficient counterions (Na$^+$) were added to make the system electroneutral. Following this, seven ions of Na$^+$ and Cl$^-$ each were added to the simulation box to yield an excess background electrolyte concentration of 25 mM.[35,36] A second system (simulation α/β-2) was set up by placing the two Pls (α and β) peptides in a parallel orientation with the C-termini of the peptides touching the upper leaflet of the bilayer. A third system (simulation α/β-3) was set up to investigate the role of GxxxG motif in mediating peptide−peptide interaction. In this system, the two peptides were placed in antiparallel orientation (same as in simulation α/β-1) and the α-peptide had two mutations, G9I and G13I. Finally, systems were also set up where α-peptide was replaced with fragment α2 (simulation α2/β) or fragment α3 (simulation α3/β) and the two peptides were in antiparallel orientation. The details of the periodic cell for each system, including the number of water molecules, lipids, and the initial box size, are listed in Table S2.

Simulation Methods and Parameters. MD simulations were performed using the GROMACS 3.33 simulation package and the GROMOS96 force field on a four-node cluster.[37,38] All systems were simulated in the isobaric isothermal (NPT) ensemble at 300 K using periodic boundary conditions. Weak coupling of the proteins to a solvent bath of constant temperature was maintained using the Berendsen thermostat with a coupling constant τ_T = 0.1 ps. The pressure was controlled using the Berendsen algorithm at 1 bar with a coupling constant τ_P = 1 ps at 300 K. For all simulations, the neighbor list was updated every 10 steps, with a neighbor list cutoff distance of 1.2 nm. The Lennard-Jones interactions were truncated at a cutoff distance of 1.2 nm. The long-range electrostatic interactions were modeled using the particle mesh Ewald (PME) summation method with a cutoff distance of 1.2 nm for the real space. The integration time step was 2 fs, and the coordinates and velocities were saved every 4 ps. The LINCS algorithm was used to restrain all bond lengths.[39] The system was energy-minimized before the MD simulation using 1000 steps of the steepest descent energy minimization method in order to relax any steric conflicts generated during the setup. The equilibration of the peptide−bilayer−water system was achieved by performing a 5 ns MD run with positional restraint on the peptide. Following this, a full MD run of 400 ns was performed without any restraints. Simulations were analyzed using various GROMACS postprocessing routines. Swiss-PdbViewer[28] and ViewerLite 5.0[40] were used to visualize and superimpose structures.

■ RESULTS

Homology Models of Plantaricin S (Pls). Multiple sequence alignment of class IIb bacteriocins revealed that some peptides have very high sequence similarity within this class of peptides. The high sequence similarity of Pls-α and Pls-β to PlnE and LcnG-β, respectively, for which the solution structure is known, allowed the use of homology-based techniques for predicting the structures of Pls peptides. The three-dimensional NMR structure of PlnE (PDB code 2JUI),[15] which has 28.9% sequence similarity with Pls-α, was used to construct homology model for Pls-α. Similarly, the NMR structure of LcnG-β[14] with 37% sequence similarity to Pls-β was used to obtain homology-based structure for Pls-β. The homology-based structures for the two Pls peptides show that both peptides are helical (Figure 1). Pls-α, a 27-residue peptide, is

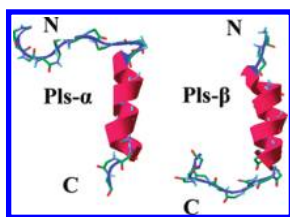**Figure 1.** Homology-based structures of the two-peptide plantaricin S (Pls-α and Pls-β). The α-helix region is shown in ribbon representation (red) and the extended coil region as loop (blue).

composed of a C-terminal α-helix that extends from residues 15 to 25 and an unstructured N-terminal part, while Pls-β, a 26-mer, has an N-terminal α-helix extending from residues 4 to 15 and an unstructured C-terminal region. Further, the secondary structure prediction[41,42] of the Pls peptides displayed the presence of helical regions as found in the homology-based structures.

Design of Pls Analogues. The two Pls peptides, Pls-α and Pls-β, contain GxxG like motifs that are believed to engage in specific interactions between the two peptides. For the GxxG motifs to interact with each other, the two peptides must form a parallel or an antiparallel helix—helix structure. To investigate this hypothesis and the importance of GxxG in peptide inter-action and activity, five peptide fragments were designed based on the sequence of the wild type Pls-α and Pls-β peptides (Table 2). These fragments were essentially N- or C-terminally truncated wild type Pls-α or Pls-β. Peptide fragments α1, α2, and α3 were derived from Pls-α, and β4 and β5 were from Pls-β. Peptide α1 is a 15-mer derived from the N-terminal region of the wild type Pls-α that contains the GxxG motif but lacks the helical region. Peptide α2, a 21-mer, consists of the GxxG motif and the helical portion of the wild type peptide, and peptide α3, a 14-residue peptide fragment, contains mainly the C-terminal helical portion of the wild type peptide.

Fragments β4 and β5 are 16-mer and 21-mer peptides, respectively, that are derived from the N-terminal region of the Pls-β peptide. Both fragments contain the AxxxA motif and the helical region from the wild type Pls-β. Fragment β5 also contains aromatic (F18) and negatively charged (E20) residues from the C-terminal region. Class IIb bacteriocins are positively charged peptides; however, a negatively charged residue is often present in their sequence. For instance, a negative charge at position 10 (D10) is present in the lactococcin G β-peptide and was found to be important for activity. Similarly, a negatively charged residue is present at position 1 (E1) of Ent-α.[25] Pls-α has no negatively charged residue, while Pls-β has two of them (D13 and E20). D13 lies within the important $A_{10}xxxA_{14}$ motif. However, the significance of the acidic residue E20 is not known. Peptide analogue β5 was designed to study the importance of the negative charge at position 20.

Synthesis of Pls and Pls Analogues. The two Pls peptides and the five designed peptide fragments were synthesized using Fmoc solid-phase peptide synthesis. The single methionine residue in Pls-α and α-peptide fragments (α1 and α2) was replaced with norleucine to avoid aerobic oxidation and confer more stability to the synthesized peptides. Peptides were purified using reversed-phase HPLC followed by characterization with MALDI-TOF mass spectrometry and analytical HPLC (Table S1 and Figure S1, Supporting Information). In general, pure peptides were obtained with an overall yield of 34—49% and purity greater than 95%.

Antibacterial Activity against Different Strains. The activity spectra of the synthetic Pls and Pls fragments were evaluated against three nonpathogenic indicator strains, namely, *C. divergens* LV13 (UAL9), *L. plantarum* (WCSF1), and *L. fermentrum* 14931. Pls (Pls-α in combination with Pls-β) displayed potent antimicrobial activity in the nanomolar range (35—100 nM) against all three indicator strains (Table 3). Fragments α2 and β5 in combination with the complementary wild-type peptide (Pls-α or Pls-β) displayed comparable potency against these strains (50—280 nM), while fragments α1, α3, and β4 did not show any activity up to 500 μM. Peptide fragment α2 contains the GxxG motif as well as the helical region from the native sequence, whereas α1 and α3 contain either the GxxG motif or the helical region in their sequences. The activity results suggest that in the α-peptide, both G_9xxxG_{13} and helical region (C-terminal) are required for activity. Fragments β5 (and not β4) in combination with the Pls-α showed activity suggesting the importance of the helical region, $A_{10}xxxA_{14}$ motif, the aromatic residue F18 and the acidic residue E20. Interestingly, α2 in combination with β5 is 1000-fold less active (50—350 μM) than the native Pls. This suggests that these two peptides do not engage in strong helix—helix interaction with each other and/or bind weakly to the putative target receptor. However, the low anti-bacterial activity of the α2-β5 pair implies that it retains the minimum pharmacophore (amino acid residues) needed for binding each other and/or the target cell membrane receptor.

The wild type Pls and the Pls fragments were also evaluated for activity against pathogenic bacteria. Analysis of the sequence similarity between class IIb and class IIa bacteriocins showed that there is a significant sequence similarity among these two classes of bacteriocins, ranging from 14% to 38% between Pls and some class IIa peptides, like curvacin A, carnobacteriocin B2, and leucocin A. This suggested that Pls could have antilisterial and antienterococcal activity similar to class IIa peptides. To test this hypothesis, four Gram-positive pathogenic strains were selected as indicator strains for the activity assay, two strains from *Enterococci* and two from *L. monocytogenes*. Wild-type Pls displayed nanomolar activity (40—350 nM) against all four pathogenic strains, while fragments α2 and β5 displayed activity in the micromolar range against some of the strains (Table 3). Peptide α2 in combination with β5 did not show any activity against the pathogenic strains up to 500 μM. The high activity of the wild-type Pls against these pathogens encouraged us to test the antibacterial activity against pathogenic *S. aureus*. Surprisingly, Pls was active against *S. aureus* ATCC 6538 and *S. aureus* ATCC 25932 in the low micromolar range (1—7 μM). These findings highlight the potential therapeutic importance of Pls against common pathogenic and food poisoning organisms. Other class IIb bacteriocins may also display similar activity which remains to be evaluated.

Next, we explored the ability of inactive peptide fragments, α1, α3, and β4 to inhibit the antimicrobial activity of the wild-type Pls. Of the three fragments, only α3 displayed significant inhibition of Pls activity against *C. divergens* in a dose-dependent manner (Figure 2). Fragments α1 and β4 did not show any inhibition of Pls activity up to 100 μM. Fragment α3 is derived from the C-terminal portion of Pls-α and spans the helical region of Pls-α, while α1 is from the N-terminal region of Pls-α. The above results indicate that the C-terminal helical region in the α-peptide may play an important role in determining cell specificity or mediating specific interaction with the β-peptide and/or the target cell membrane receptor. Fragment β4 that

Table 3. Antibacterial Activity of Pls and Fragments against Nonpathogenic (Top Three) and Pathogenic Indicator Strains

	MIC[a] of peptides (nM)			
indicator strains	Pls-α/Pls-β	α2/Pls-β	Pls-α/β5	α2/β5
C. divergens LV13	35 ± 3	80 ± 6	50 ± 4	$5 \times 10^4 \pm 5000$
L. plantarum (WCSF1)	90 ± 8	175 ± 13	250 ± 14	$2 \times 10^5 \pm 11000$
L. fermentrum ATCC 14931	100 ± 9	220 ± 12	280 ± 17	$3.5 \times 10^5 \pm 15000$
E. faecalis ATCC 19433	50 ± 4	$1 \times 10^5 \pm 8000$	$6 \times 10^4 \pm 5000$	−
E. faecium ATCC 19434	250 ± 12		$2 \times 10^5 \pm 12000$	−
L. monocytogenes NCTC 5105.3	40 ± 3	$8 \times 10^4 \pm 7000$	$5 \times 10^4 \pm 4000$	−
L. monocytogenes CDC 7762[b]	350 ± 18	−	−	−
S. aureus ATCC 6538	1000 ± 200	ND	ND	ND
S. aureus ATCC 25932	7000 ± 800	ND	ND	ND

[a] Activity was quantified in terms of the MICs of the two peptides (the sum of the concentrations of the two complementary peptides at a 1:1 ratio) measured against the indicator strains. −, no activity was detected up to 5×10^5 nM. ND, not determined. Data are the mean ± standard error of the mean. The values are results of at least three independent measurements. [b] An outbreak isolate strain.
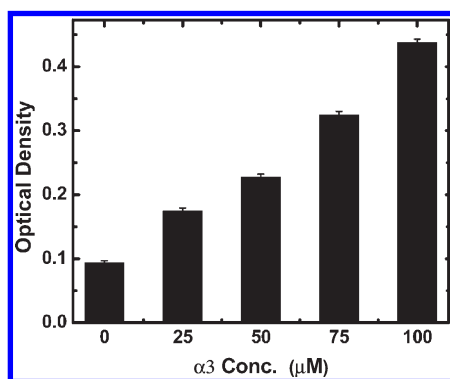

Figure 2. Dose dependent decrease in antimicrobial activity of Pls (Pls-α/Pls-β, 1:1) in the presence of α3 against *C. divergens* LV13. Antimicrobial activity is expressed as optical density at 600 nm ± standard deviation.

Figure 3. Circular dichroism (CD) spectra of Pls-α, Pls-β, Pls (Pls-α in combination with Pls-β, 1:1, premixed) (upper panel) and fragments α2 and α3 (lower panel) in 50% aqueous TFE containing 0.05% TFA.

spans the helical region of Pls-β but lacks the C-terminal E20 residue did not show any bacteriocin inhibitory activity. This may indicate that the C-terminal negative charge of Pls-β is important for docking the β-peptide on the α-peptide or on the target cell surface. The interaction of the two Pls peptides with cell membrane could be sequential as observed for the lactococcin G, where one peptide binds first followed by the addition of the complementary peptide to display activity.[12]

Structure–Activity Relationship. *Solution Conformation using CD Spectroscopy.* Several studies have pointed out the importance of helical secondary structure in class IIa and class IIb bacteriocins in mediating the antibacterial activity.[8,19,23] Homology-based structures of Pls-α and Pls-β show the presence of α-helix in both peptides (Figure 1). To further confirm whether Pls peptides have definitive secondary structure elements that may contribute to its antibacterial activity, the solution conformations of Pls and Pls-derived fragments were studied using CD spectroscopy. The spectra were obtained in 50% TFE/water mixture for each peptide. As shown in Figure 3, all individual peptides and Pls (Pls-α in combination with Pls-β) displayed characteristic peaks for the helical structure. It is known that these peptides are unstructured in water, and TFE induces helical structure.[43,44] Spectra were obtained in 50% TFE, and a further increase in TFE concentration did not increase the helical content. CD spectra for each peptide were collected at three
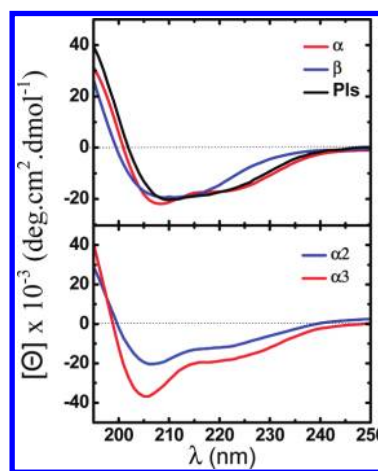
different concentrations (25, 50, and 100 uM). The spectra were found to be independent of concentration, suggesting that peptides do not aggregate in this concentration range.

The quantitative analysis of the CD data using CDPRO software[26] revealed the relative helical content in Pls peptides and the fragments. The helical content in the presence of 50% TFE in Pls-α peptide was 39.9 ± 0.9%, whereas in Pls-β, it was 29 ± 0.6%. Interestingly, premixing the α and β peptides prior to CD scan resulted in 39.6 ± 1% helical content, which is 5% higher than the content calculated based on the individual spectra of Pls-α and Pls-β. This suggests that the α and β peptides may be involved in direct interaction (pairing) with each other in a structure-inducing manner as observed previously for lactococcin G, plantaricin E/F, and plantaricin J/K.[19,45] Peptide fragments α2 and α3 also displayed high helical content (32.3% and 46.7%, respectively), which is in good agreement with the homology models that are created (vide infra). The high helical content of α3 (46.7%) supports the potential role of the helical structure in mediating specific interaction with the complementary peptide and/or target cell membrane.

MD Simulation. MD simulations were used to study the interaction of Pls peptides (Pls-α with Pls-β) with each other and with a model lipid bilayer. Two different orientations for the
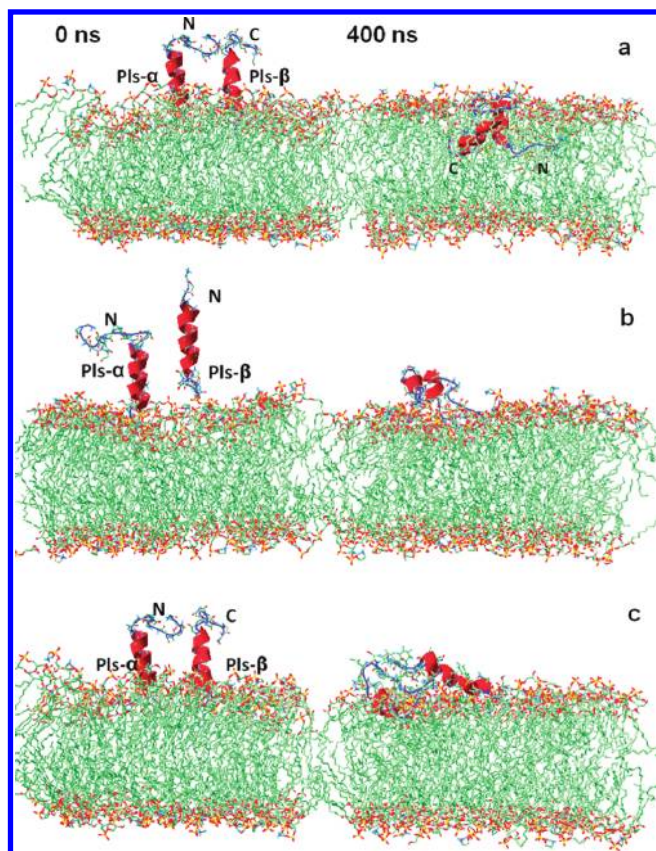
Figure 4. Snapshots from simulations (a) α/β-1, (b) α/β-2, and (c) α/β-3 at 0 and 400 ns illustrating the interaction of Pls-α and Pls-β peptides with each other and with the model lipid bilayer. The two peptides were placed in an antiparallel orientation (simulations α/β-1 and α/β-3) or in a parallel orientation (simulation α/β-2) in z direction perpendicular to the plane of the bilayer. In simulation α/β-3, G_9xxxG_{13} of Pls-α is substituted with I_9xxxI_{13}.

α- and β-peptide interaction (pairing) were explored, namely, antiparallel (simulation α/β-1) and parallel (simulation α/β-2) as shown in Figure 4. Both these orientations have been proposed previously for the other two-peptide class IIb bacteriocins.[16,17] Another simulation, simulation α/β-3, where the G_9xxxG_{13} motif in Pls-α was substituted with I_9xxxI_{13}, was also conducted. It has been shown that motifs like GxxxG from each peptide are involved in peptide−peptide interaction, and this interaction is important for activity.[17] Previously Moll et al. revealed that lactococcin G displays optimal antibacterial activity at 1:1 stoichiometry,[11] and whether the active form of these peptides is dimer, tetramer, or higher complex is not clear yet. In this regard, we conducted simulations of higher multimers (tetramer and hexamer) of Pls. However, because of the high cationic nature of these peptides, repulsion between pairs of Pls was observed and no stable complex was detected with higher multimers.

Peptide−Peptide and Peptide−Bilayer Interaction. Simulations α/β-1 and α/β-2 were conducted for 400 ns, and the results from these simulations indicate that the antiparallel orientation of Pls-α and Pls-β peptides is the preferred orientation in which these two peptides pair up and interact. First, we examined the trajectories from the two simulations. During simulation α/β-1, the two peptides approached each other as early as 5−10 ns. Specifically, the helical regions from the two

peptides and the GxxxG motif in α-peptide and AxxxA motif in β-peptide came close to each other. Subsequently, the peptides inserted into the upper bilayer leaflet with their relative orientation remaining almost the same. Toward the end of the simulation, the helical regions of both the peptides became completely inserted in the bilayer with their termini interacting with the polar headgroups of the upper bilayer leaflet (Figure 4a). This insertion of the peptides into the bilayer surface as a function of time is plotted in Figure S2a. Peptides start inserting into the bilayer at around 180−200 ns. In the parallel orientation (simulation α/β-2, Figure 4b), the two peptides come close to each other and to the bilayer surface. However, there was a loss in secondary structure and peptides do not insert into the bilayer (Figure S2a). Only few polar residues (terminal lysine residues from Pls-α as well as E20 and N24 from Pls-β) interact with the bilayer head groups. A partial loss of helical structure (19.3% instead of 40% helix in the starting structure) during simulation α/β-2 was observed, contrary to the structure inducing behavior found in LcnG peptides when premixed and exposed to liposomes.[19] Figure S2b shows that as the simulation advanced, the conserved motifs from the two peptides (G_9xxxG_{13} of Pls-α and $A_{10}xxxA_{14}$ of Pls-β) approached each other equilibrating at a distance of 0.5 $\pm$ 0.02 and 0.7 $\pm$ 0.038 nm, respectively, for simulations α/β-1 and α/β-2. After 150 ns, these distances were maintained for the remainder of the simulations. The shorter distance between the conserved motifs from the two peptides during simulation α/β-1 suggests strong interaction in the antiparallel orientation.

A closer look at the specific interaction between the GxxxG and AxxxA motifs during simulation α/β-1 shows how these motifs align with each other (Figure S3). There were five to seven hydrogen bonds between Pls-α and Pls-β involving residues G9, H10 from Pls-α and D13 from Pls-β, emphasizing the role of the two motifs in stabilizing the helix−helix interaction in Pls. In addition, K3, L4, Y6, N7, M8 from Pls-α and A14, S17, E20 from Pls-β also participated in the hydrogen bond formation. Residue E20 from Pls-β was always engaged in hydrogen bonding with the bilayer head groups, while F18 aligned at the bilayer−water interface. These findings highlight the importance of F18 and E20 residues in positioning Pls-β with regard to the bilayer surface. Such behavior of aromatic and charged residues has been reported previously.[34,46] In contrast, for simulation α/β-2 no stable hydrogen bonds were detected.

To investigate the role of the G_9xxxG_{13} motif in Pls-α in mediating peptide−peptide interaction prior to bilayer insertion, G9 and G13 were substituted with isoleucine (simulation α/β-3, Figure 4c). Such mutation in lactococcin G resulted in a detrimental effect on antimicrobial activity.[17] Analysis of the trajectories of simulation α/β-3 showed that the peptides moved to the surface of bilayer, as shown in Figures 4c and S2a, and interacted with the bilayer electrostatically. However, strong interaction between the Pls-α and Pls-β was not observed. During the first 50 ns, the I_9xxxI_{13} motif of Pls-α came close to the $A_{10}xxxA_{14}$ of Pls-β (Figure S2b). These motifs from the two peptides, however, maintained a distance of 1.3 $\pm$ 0.04 nm, suggesting that the two peptides do not interact strongly.

Finally, we compared the potential energies for the two systems corresponding to different orientations (antiparallel and parallel) of the peptides relative to the bilayer. The excess energies were calculated as described previously.[34] Simulation α/β-1, where the two Pls peptides are in antiparallel orientation and get inserted into the bilayer upon equilibration, attains lower energy (−3718 kJ/mol) compared to simulation α/β-2 with
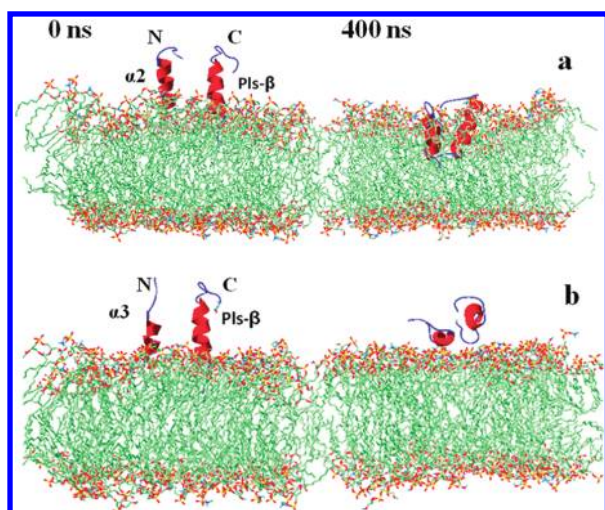
Figure 5. Snapshots of simulations (a) α2/β and (b) α3/β at 0 and 400 ns. Peptides α2 and α3 are fragments derived from Pls-α. These peptide fragments were allowed to interact with the Pls-β in the same starting orientation as in simulation α/β-1.

peptides in parallel orientation (−643 kJ/mol). Thus, the two Pls peptides in antiparallel orientation are energetically more favorable. Overall, the above results suggest that the antiparallel orientation is likely the preferred orientation in which the two Pls peptides interact and display activity.

Peptide Fragments. Peptide fragment α2 in combination with Pls-β displayed antibacterial activity comparable to that of the wild-type Pls, while the α3/Pls-β combination was inactive. In order to understand such behavior, two MD simulation systems, simulations α2/β and α3/β, were set up to study the interaction of fragments α2 or α3 with the complementary Pls-β peptide (Figure 5).

During simulation α2/β, the two peptides were involved in strong helix−helix interaction mediated by G_9xxxG_{13} and $A_{10}xxxA_{14}$ motifs along with insertion into the bilayer. Several stable hydrogen bonds between the two peptides were detected, which stabilized the two peptides and presumably enabled them to move gradually toward the bilayer core. The pattern of the hydrogen bonds between the two peptides and the membrane was similar to that in simulation α/β-1 (data not shown). The movement of the two peptides toward the bilayer core was observed at around 250 ns, which is much slower compared to that observed during simulation α/β-1 (Figure S4a). The GxxxG and AxxxA motifs come in close contact, approaching a distance of about 0.78 ± 0.03 nm toward the end of the simulation (300−400 ns, Figure S4b). These findings highlight the helix−helix interaction, interaction between the GxxxG type motifs, and peptides insertion into the bilayer during simulation α2/β (Figure S4) and α/β-1 (Figure S2) and suggest that these may play an important role in the toxicity of Pls-α and α2 peptides.

During simulation α3/β, the two peptides come slightly closer (from the starting distance at t=0 ns) to the surface of the bilayer (Figure S4a) and maintain a distance of about 0.87 ± 0.04 nm from the bilayer surface. Peptide α3 came in close contact with the bilayer compared to Pls-β, and both peptides adopt a parallel orientation with respect to the bilayer. Some helix−helix interaction between the two peptides (α3/Pls-β) was observed. However, no stable hydrogen bonds were detected during the entire simulation. These results suggest that α3, which lacks the important G_9xxxG_{13} motif, is unable to engage in strong peptide−peptide interaction which seems important for bilayer insertion and membrane toxicity.

■ DISCUSSION

Class IIb bacteriocins display potent activity against several bacteria. However, as observed for the bacteriocins from other classes (such as class IIa bacteriocins), these AMPs have a narrow activity spectrum and display activity against only closely related species. In this regard, class IIa bacteriocins are often referred to as antilisterial peptides, as they display potent activity against *Listerium* species. There is a huge interest in making these bacteriocins broad spectrum to increase their potential in food industry and pharmaceutical applications. We found that the sequence homology in the C-terminal region of class IIa and class IIb is up to 38%, and it has been shown that class IIa bacteriocins acquire the target cell specificity from the C-terminal domain.[47] On the basis of this observation, the antimicrobial activity of class IIb bacteriocin was evaluated against a variety of class IIa bacteriocin sensitive pathogens. Interestingly, Pls showed potent activity against four pathogens; one of them (*L. monocytogenes* CDC 7762) is an outbreak isolate from hospital settings. In addition, Pls displayed micromolar activity against *S. aureus*. This is the first report to show the potent antilisterial activity of a two-peptide class IIb bacteriocin. These results further suggest that class IIa bacteriocins in combination with class IIb (β-peptide of the two-peptide bacteriocin) may display broader activity spectrum, and the activity of such classIIa/IIb peptide combinations is being evaluated.

Class IIb bacteriocins not only display sequence similarity with class IIa bacteriocins but also behave similarly with respect to solution conformation. The CD and NMR studies reveal that class IIa and class IIb peptides are unstructured in water and become structured when in membrane mimicking solvents.[19,48−52] The NMR solution structures of three two-peptide bacteriocins show that the individual peptides fold into helical conformation in TFE or DPC micelles. Utilizing the NMR structures, we obtained homology-based structures for Pls (Figure 1) to study structure−activity relationships among these peptides. Homology-based structure determination of peptides is a facile method to predict the solution conformation of peptides for which the NMR structure is not yet available.[23] This technique has been used widely, and the availability of homology-based structure facilitates the study of peptide interaction and dynamics using MD simulations. MD simulations were used to study the interaction of a representative two-peptide bacteriocin Pls with a mixed (anionic−zwitterionic) bilayer model representing cell membrane of Gram-positive bacteria (Table S2). Two different orientations, parallel and antiparallel, for the α/β-pair were explored (Figure 4), as these orientations have been proposed for other class IIb bacteriocins.[16,17] Oppegard et al. have suggested a parallel orientation of the two complementary peptides (LcnG-α and LcnG-β) to be the preferred orientation for interaction in two-peptide bacteriocin lactococcin G.[17] However, Ronge et al. showed that both orientations could be possible for another two-peptide bacteriocin, plantaricin JK.[16] Our results show that Pls peptides orient themselves in an antiparallel fashion for helix−helix interaction and interaction with the bilayer (Figures 4 and S2). More studies are certainly required to elucidate the mechanism of interactions among different class IIb bacteriocins.

The GxxxG motifs and the helical region in class IIb bacteriocins have been considered important for interpeptide helix helix interaction and disruption of target cell membrane. For instance, the importance of GxxxG motifs for antimicrobial activity of LcnG has been reported.[15,17] Substitution of the glycine residues with large hydrophobic amino acids (Ile or Leu) inactivated LcnG. We found that fragment α3 (α3 in combination with Pls-β) that contains the C-terminal helical region from wild type Pls-α and does not contain the GxxxG motif was inactive. Interestingly, α3 was able to compete with Pls-α in a competitive inhibition experiment (Figure 2), suggesting that the helical region is important for specific recognition by the Pls-β and/or target cell membrane. When both the GxxxG motif and the helix are present in the sequence, the peptide (α2 in combination with Pls-β) displays potent antimicrobial activity. Similarly, structure–function analyses of the pediocin-like (class IIa) bacteriocins revealed that the helical region is involved in determining the antimicrobial specificities.[46] A peptide fragment that spans the helical region of class IIa pediocin PA-1 specifically inhibited the antibacterial activity of pediocin PA-1.[53] Several other studies revealed that the helical interactions between peptide bacteriocins and integrated membrane (transport) proteins might be a common mechanism whereby peptide bacteriocins cause membrane leakage.[21,54−56]

Finally, substitution of G_9xxxG_{13} motif in Pls-α to I_9xxxI_{13} (simulation α/β-3) showed similar behavior as the fragment α3 which lacks the GxxxG motif. During both simulations (simulations α/β-3 and α1/β), the peptides showed very little interaction with the complementary β-peptide (Pls-β). Also, no insertion in the bilayer was observed. The different interaction behavior of Pls in simulation α/β-3 compared to simulation α/β-1 could be due to the presence of the large hydrophobic isoleucine residues between the two helices compared to glycine residues in the wild-type Pls. This prevented the peptides from coming too close to each other, and the I_9xxxI_{13} motif from Pls-α and AxxxA motif from Pls-β maintained a distance of 1.3 ± 0.04 nm from each other (Figure S2b).

■ CONCLUDING REMARKS

Earlier studies have shown that class IIb bacteriocins, similar to class IIa, display activity against closely related bacteria. Class IIa or pediocin-like bacteriocins are antilisterial peptides that have high sequence similarly with class IIb bacteriocins. This prompted us to examine the antibacterial activity of a representative class IIb bacteriocin, Pls against pathogens like *L. monocytogenes* and *E. faecalis*. We found that Pls displays high potency (nanomolar) against these pathogens. Moreover, Pls showed low micromolar activity against two pathogenic *S. aureus* strains and further studies could reveal more strains that are sensitive to Pls. The current use of bacteriocins is limited to food preservation and animal feed; however, our results shed light on the potential therapeutic use of class IIb bacteriocins as an alternative to conventional antibiotics. The results broaden the activity spectrum of class IIb bacteriocins and highlight the fact that these peptides may have similar mechanism of action as class IIa bacterioicins.

Two peptide fragments (α2 and β5), which span the helical region of wild type Pls and contain the important GxxxG and AxxxA motifs, respectively, displayed antibacterial activity against nonpathogenic strains that is comparable to wild-type Pls. The high helical content of the synthesized peptides as inferred from the homology modeling and confirmed by CD spectroscopy and MD simulations emphasizes the role of α-helix secondary structure as an important structural motif in this class of peptides. The importance of the helical region in class IIb and class IIa bacteriocins has been emphasized previously.[19] Further the ability of fragment α3 to act as a competitive inhibitor of wild-type Pls indicates the presence of a membrane docking entity or potential receptor protein on target cells as suggested previously for lactococcin G.[17,20] Our results indicate that the helical regions together with the conserved GxxxG and AxxxA motifs mediate helix–helix interaction between the two peptides prior to membrane insertion. This likely serves as an initial step for binding to a membrane docking entity/receptor embedded in the membrane of sensitive cells. Removal of the N-terminal region of Pls-α (α2) and C-terminal part of Pls-β (β5) resulted in an incomplete pairing of the two peptides which may lead to incomplete fitting with the potential target cell receptor. However, these fragments still retain the antibacterial activity against closely related nonpathogenic strains. Detailed studies on the interaction of Pls with a membrane model are currently in progress which will reveal more insight on the different aspects of interaction of this class of peptides with target cells. Such insight will be valuable for future rational design of bacteriocin variants with properties that will make them useful for medical and biotechnological applications.

■ ASSOCIATED CONTENT

Ⓢ **Supporting Information.** Additional Tables (S1, S2) and Figures (S1−S4) related to peptide purification, characterization, and MD simulations. This material is available free of charge via the Internet at http://pubs.acs.org.

■ AUTHOR INFORMATION

Corresponding Author
*Phone: 780-492-8917. Fax: 780-492-1217. E-mail: kkaur@ualberta.ca.

■ ACKNOWLEDGMENT

■ ABBREVIATIONS USED

AMP, antimicrobial peptide; ABC, ATP-binding cassette; CD, circular dichroism; DIC, 1,3-diisopropylcarbodiimide; Fmoc, 9-fluorenylmethyloxycarbonyl; DPC, dodecylphosphocholine; HOBt, *N*-hydroxybenzotriazole; HPLC, high performance liquid chromatography; LAB, lactic acid bacteria; MALDI-TOF, matrix-assisted laser desorption ionization time of flight; MD, molecular dynamics; MIC, minimum inhibitory concentration; ND, not determined; NMR, nuclear magnetic resonance; PDB, Protein Data Bank; PME, particle mesh Ewald; POPE, palmitoyloleoylphosphatidylethanolamine; POPG, palmitoyloleoylphosphatidylglycerol; TFA, trifluoroacetic acid; TFE, 2,2,2-trifluoroethanol

■ REFERENCES

(1) Nissen-Meyer, J.; Rogne, P.; Oppegard, C.; Haugen, H. S.; Kristiansen, P. E. Structure−function relationships of the non-lanthionine-containing peptide (class ii) bacteriocins produced by Gram-positive bacteria. *Curr. Pharm. Biotechnol.* **2009**, *10*, 19–37.

(2) Cotter, P. D.; Hill, C.; Ross, R. P. Bacteriocins: developing innate immunity for food. *Nat. Rev. Microbiol.* **2005**, *3*, 777–788.

(3) Stiles, M. E. Secondary Carnobacterium CB1, CB2, and CB3. U. S. Appl. US2005019458 (A1), 2005.

(4) Stiles, M. E.; McMullen, L. M.; Smith, D. C. Secondary Enhanced Preservation of Processed Food. Patent Appl. WO2007106993 (A1), 2007.

(5) Stiles, M. E.; McMullen, L. M.; Smith, D. C. Secondary Lactic Acid Bacteria for the Treatment of Food. Patent Appl. WO2006063428 (A1), 2007.

(6) Corr, S. C.; Li, Y.; Riedel, C. U.; O'Toole, P. W.; Hill, C.; Gahan, C. G. Bacteriocin production as a mechanism for the antiinfective activity of *Lactobacillus salivarius* UCC118. *Proc. Natl. Acad. Sci. U.S.A.* **2007**, *104*, 7617–7621.

(7) Oppegard, C.; Rogne, P.; Emanuelsen, L.; Kristiansen, P. E.; Fimland, G.; Nissen-Meyer, J. The two-peptide class II bacteriocins: structure, production, and mode of action. *J. Mol. Microbiol. Biotechnol.* **2007**, *13*, 210–219.

(8) Nissen-Meyer, J.; Oppegard, C.; Rogne, P.; Haugen, H. S.; Kristiansen, P. E. Structure and mode-of-action of the two-peptide (class-IIb) bacteriocins. *Probiotics Antimicrob. Proteins* **2010**, *2*, 52–60.

(9) Castellano, P.; Raya, R.; Vignolo, G. Mode of action of lactocin 705, a two-component bacteriocin from *Lactobacillus casei* CRL705. *Int. J. Food Microbiol.* **2003**, *85*, 35–43.

(10) Cuozzo, S. A.; Castellano, P.; Sesma, F. J.; Vignolo, G. M.; Raya, R. R. Differential roles of the two-component peptides of lactocin 705 in antimicrobial activity. *Curr. Microbiol.* **2003**, *46*, 180–183.

(11) Moll, G.; Ubbink-Kok, T.; Hildeng-Hauge, H.; Nissen-Meyer, J.; Nes, I. F.; Konings, W. N.; Driessen, A. J. Lactococcin G is a potassium ion-conducting, two-component bacteriocin. *J. Bacteriol.* **1996**, *178*, 600–605.

(12) Moll, G.; Hildeng-Hauge, H.; Nissen-Meyer, J.; Nes, I. F.; Konings, W. N.; Driessen, A. J. Mechanistic properties of the two-component bacteriocin lactococcin G. *J. Bacteriol.* **1998**, *180*, 96–99.

(13) Moll, G. N.; van den Akker, E.; Hauge, H. H.; Nissen-Meyer, J.; Nes, I. F.; Konings, W. N.; Driessen, A. J. Complementary and overlapping selectivity of the two-peptide bacteriocins plantaricin EF and JK. *J. Bacteriol.* **1999**, *181*, 4848–4852.

(14) Rogne, P.; Fimland, G.; Nissen-Meyer, J.; Kristiansen, P. E. Three-dimensional structure of the two peptides that constitute the two-peptide bacteriocin lactococcin G. *Biochim. Biophys. Acta* **2008**, *1784*, 543–554.

(15) Fimland, N.; Rogne, P.; Fimland, G.; Nissen-Meyer, J.; Kristiansen, P. E. Three-dimensional structure of the two peptides that constitute the two-peptide bacteriocin plantaricin EF. *Biochim. Biophys. Acta, Proteins Proteomics* **2008**, *1784*, 1711–1719.

(16) Rogne, P.; Haugen, C.; Fimland, G.; Nissen-Meyer, J.; Kristiansen, P. E. Three-dimensional structure of the two-peptide bacteriocin plantaricin JK. *Peptides* **2009**, *30*, 1613–1621.

(17) Oppegard, C.; Schmidt, J.; Kristiansen, P. E.; Nissen-Meyer, J. Mutational analysis of putative helix−helix interacting GxxxG-Motifs and tryptophan residues in the two-peptide bacteriocin lactococcin G. *Biochemistry* **2008**, *47*, 5242–5249.

(18) Oppegard, C.; Rogne, P.; Kristiansen, P. E.; Nissen-Meyer, J. Structure analysis of the two-peptide bacteriocin lactococcin G by introducing D-amino acid residues. *Microbiology* **2010**, *156*, 1883–1889.

(19) Hauge, H. H.; Nissen-Meyer, J.; Nes, I. F.; Eijsink, V. G. Amphiphilic alpha-helices are important structural motifs in the alpha and beta peptides that constitute the bacteriocin lactococcin G—enhancement of helix formation upon alpha-beta interaction. *Eur. J. Biochem.* **1998**, *251*, 565–572.

(20) Oppegard, C.; Emanuelsen, L.; Thorbek, L.; Fimland, G.; Nissen-Meyer, J. The lactococcin g immunity protein recognizes specific regions in both peptides constituting the two-peptide bacteriocin lactococcin g. *Appl. Environ. Microbiol.* **2010**, *76*, 1267–1273.

(21) Diep, D. B.; Skaugen, M.; Salehian, Z.; Holo, H.; Nes, I. F. Common mechanisms of target cell recognition and immunity for class II bacteriocins. *Proc. Natl. Acad. Sci. U.S.A.* **2007**, *104*, 2384–2389.

(22) Jimenez-Diaz, R.; Ruiz-Barba, J. L.; Cathcart, D. P.; Holo, H.; Nes, I. F.; Sletten, K. H.; Warner, P. J. Purification and partial amino acid sequence of plantaricin S, a bacteriocin produced by *Lactobacillus plantarum* LPCO10, the activity of which depends on the complementary action of two peptides. *Appl. Environ. Microbiol.* **1995**, *61*, 4459–4463.

(23) Kaur, K.; Andrew, L. C.; Wishart, D. S.; Vederas, J. C. Dynamic relationships among type IIa bacteriocins: temperature effects on antimicrobial activity and on structure of the C-terminal amphipathic alpha helix as a receptor-binding region. *Biochemistry* **2004**, *43*, 9009–9020.

(24) Nissen-Meyer, J.; Holo, H.; Havarstein, L. S.; Sletten, K.; Nes, I. F. A novel lactococcal bacteriocin whose activity depends on the complementary action of two peptides. *J. Bacteriol.* **1992**, *174*, 5686–5692.

(25) Oppegard, C.; Fimland, G.; Thorbaek, L.; Nissen-Meyer, J. Analysis of the two-peptide bacteriocins lactococcin G and enterocin 1071 by site-directed mutagenesis. *Appl. Environ. Microbiol.* **2007**, *73*, 2931–2938.

(26) Sreerama, N.; Woody, R. W. Estimation of protein secondary structure from circular dichroism spectra: comparison of CONTIN, SELCON, and CDSSTR methods with an expanded reference set. *Anal. Biochem.* **2000**, *287*, 252–260.

(27) http://www.ebi.ac.uk/Tools/em-boss/align/index.html.

(28) Guex, N.; Peitsch, M. C. SWISS-MODEL and the Swiss-PdbViewer: an environment for comparative protein modeling. *Electrophoresis* **1997**, *18*, 2714–2723.

(29) Epand, R. F.; Savage, P. B.; Epand, R. M. Bacterial lipid composition and the antimicrobial efficacy of cationic steroid compounds (Ceragenins). *Biochim. Biophys. Acta* **2007**, *1768*, 2500–2509.

(30) Epand, R. F.; Schmitt, M. A.; Gellman, S. H.; Epand, R. M. Role of membrane lipids in the mechanism of bacterial species selective toxicity by two alpha/beta-antimicrobial peptides. *Biochim. Biophys. Acta* **2006**, *1758*, 1343–1350.

(31) Zhao, W.; Rog, T.; Gurtovenko, A. A.; Vattulainen, I.; Karttunen, M. Atomic-scale structure and electrostatics of anionic palmitoyloleoylphosphatidylglycerol lipid bilayers with Na^+ counterions. *Biophys. J.* **2007**, *92*, 1114–1124.

(32) Elmore, D. E. Molecular dynamics simulation of a phosphatidylglycerol membrane. *FEBS Lett.* **2006**, *580*, 144–148.

(33) Tieleman, D. P.; Forrest, L. R.; Sansom, M. S.; Berendsen, H. J. Lipid properties and the orientation of aromatic residues in OmpF, influenza M2, and alamethicin systems: molecular dynamics simulations. *Biochemistry* **1998**, *37*, 17554–17561.

(34) Soliman, W.; Bhattacharjee, S.; Kaur, K. Interaction of an antimicrobial peptide with a model lipid bilayer using molecular dynamics simulation. *Langmuir* **2009**, *25*, 6591–6595.

(35) Boziaris, I. S.; Skandamis, P. N.; Anastasiadi, M.; Nychas, G. J. Effect of NaCl and KCl on fate and growth/no growth interfaces of Listeria monocytogenes Scott A at different pH and nisin concentrations. *J. Appl. Microbiol.* **2007**, *102*, 796–805.

(36) Delgado, A.; Arroyo Lopez, F. N.; Brito, D.; Peres, C.; Fevereiro, P.; Garrido-Fernandez, A. Optimum bacteriocin production by *Lactobacillus plantarum* 17.2b requires absence of NaCl and apparently follows a mixed metabolite kinetics. *J. Biotechnol.* **2007**, *130*, 193–201.

(37) Lindahl, E.; Hess, B.; van der Spoel, D. GROMACS 3.0: a package for molecular simulation and trajectory analysis. *J. Mol. Model.* **2001**, *7*, 306–317.

(38) Spoel, D. V.; vanBuuren, A. R.; Apol, E.; Meulenhoff, P. J.; Tieleman, D. P.; Sijbers, A. L. T. M.; Hess, B.; Feenstra, K. A.; Lindahl, E.; vanDrunen, R.; Berendsen, H. J. C. Gromacs User Manual, version 3.1.1; Nijenborgh 4, 9747 AG Groningen, The Netherlands, 2002; www.gromacs.org.

(39) Hess, B.; Bekker, B.; Berendsen, H. J. C.; Fraaije, J. G. E. M. *SecondaryLINCS: A Linear Constraint Solver for Molecular Simulations*; University of Groningen: Groningen, The Netherlands, 1997; Vol. 18, pp 1463–1472.

(40) MSI, Molecular Simulations Inc., 1998.

(41) Rost, B.; Yachdav, G.; Liu, J. The PredictProtein server. *Nucleic Acids Res.* **2004**, *32*, W321–W326.

(42) Cole, C.; Barber, J. D.; Barton, G. J. The Jpred 3 secondary structure prediction server. *Nucleic Acids Res.* **2008**, *36*, W197–W201.

(43) Sonnichsen, F. D.; Van Eyk, J. E.; Hodges, R. S.; Sykes, B. D. Effect of trifluoroethanol on protein secondary structure: an NMR and CD study using a synthetic actin peptide. *Biochemistry* **1992**, *31*, 8790–8798.

(44) Jasanoff, A.; Fersht, A. R. Quantitative determination of helical propensities from trifluoroethanol titration curves. *Biochemistry* **1994**, *33*, 2129–2135.

(45) Hauge, H. H.; Mantzilas, D.; Eijsink, V. G.; Nissen-Meyer, J. Membrane-mimicking entities induce structuring of the two-peptide bacteriocins plantaricin E/F and plantaricin J/K. *J. Bacteriol.* **1999**, *181*, 740–747.

(46) Fimland, G.; Eijsink, V. G.; Nissen-Meyer, J. Mutational analysis of the role of tryptophan residues in an antimicrobial peptide. *Biochemistry* **2002**, *41*, 9508–9515.

(47) Johnsen, L.; Fimland, G.; Nissen-Meyer, J. The C-terminal domain of pediocin-like antimicrobial peptides (class IIa bacteriocins) is involved in specific recognition of the C-terminal part of cognate immunity proteins and in determining the antimicrobial spectrum. *J. Biol. Chem.* **2005**, *280*, 9243–9250.

(48) Gallagher, N. L. F.; Sailer, M.; Niemczura, W. P.; Nakashima, T. T.; Stiles, M. E.; Vederas, J. C. Three-dimensional structure of leucocin A in trifluoroethanol and dodecylphophocholine micelles: spatial location of residues critical for biological activity in type IIa bacteriocins from lactic acid bacteria. *Biochemistry* **1997**, *36*, 15062–15072.

(49) Wang, Y. J.; Henz, M. E.; Gallagher, N. L. F.; Chai, S. Y.; Gibbs, A. C.; Yan, L. Z.; Stiles, M. E.; Wishart, D. S.; Vederas, J. C. Solution structure of carnobacteriocin B2 and implications for structure–activity relationships among type IIa bacteriocins from lactic acid bacteria. *Biochemistry* **1999**, *38*, 15438–15447.

(50) Watson, R. M.; Woody, R. W.; Lewis, R. V.; Bohle, D. S.; Andreotti, A. H.; Ray, B.; Miller, K. W. Conformational changes in pediocin AcH upon vesicle binding and approximation of the membrane-bound structure in detergent micelles. *Biochemistry* **2001**, *40*, 14037–14046.

(51) Papathanasopoulos, M. A.; Dykes, G. A.; Revol-Junelles, A. M.; Delfour, A.; von Holy, A.; Hastings, J. W. Sequence and structural relationships of leucocins A-, B- and C-TA33a from *Leuconostoc mesenteroides* TA33a. *Microbiology* **1998**, *144* (Part 5), 1343–1348.

(52) Fleury, Y.; Dayem, M. A.; Montagne, J. J.; Chaboisseau, E.; Le Caer, J. P.; Nicolas, P.; Delfour, A. Covalent structure, synthesis, and structure–function studies of mesentericin Y 105(37), a defensive peptide from Gram-positive bacteria *Leuconostoc mesenteroides*. *J. Biol. Chem.* **1996**, *271*, 14421–14429.

(53) Fimland, G.; Jack, R.; Jung, G.; Nes, I. F.; Nissen-Meyer, J. The bactericidal activity of pediocin PA-1 is specifically inhibited by a 15-mer fragment that spans the bacteriocin from the center toward the C terminus. *Appl. Environ. Microbiol.* **1998**, *64*, 5057–5060.

(54) Kjos, M.; Nes, I. F.; Diep, D. B. Class II one-peptide bacteriocins target a phylogenetically defined subgroup of mannose phosphotransferase systems on sensitive cells. *Microbiology* **2009**, *155*, 2949–2961.

(55) Ramnath, M.; Arous, S.; Gravesen, A.; Hastings, J. W.; Hechard, Y. Expression of mptC of *Listeria monocytogenes* induces sensitivity to class IIa bacteriocins in *Lactococcus lactis*. *Microbiology* **2004**, *150*, 2663–2668.

(56) Drider, D.; Fimland, G.; Hechard, Y.; McMullen, L. M.; Prevost, H. The continuing story of class IIa bacteriocins. *Microbiol. Mol. Biol. Rev.* **2006**, *70*, 564–582.